

Optics Letters

Optical channel de-aggregation of quadrature-phase-shift-keying and eight-phase-shift-keying data using mapping onto constellation axes

MORTEZA ZIYADI,^{1,*} AMIRHOSSEIN MOHAJERIN-ARIAEI,¹ AHMED ALMAIMAN,¹ YINWEN CAO,¹ MOHAMMAD REZA CHITGARHA,¹ LOUKAS PARASCHIS,² MOSHE TUR,³ CARSTEN LANGROCK,⁴ MARTIN M. FEJER,⁴ JOSEPH D. TOUCH,⁵ AND ALAN E. WILLNER¹

¹Department of Electrical Engineering, University of Southern California, California 90089, USA

²Cisco Systems, 170 W. Tasman Drive, San Jose, California 95134, USA

³School of Electrical Engineering, Tel Aviv University, Ramat Aviv 69978, Israel

⁴Edward L. Ginzton Laboratory, 348 Via Pueblo Mall, Stanford University, Stanford, California 94305, USA

⁵Information Sciences Institute, University of Southern California, California 90292, USA

*Corresponding author: ziyadi@usc.edu

Received 18 August 2015; revised 20 September 2015; accepted 27 September 2015; posted 28 September 2015 (Doc. ID 248072); published 20 October 2015

An eight-phase-shift-keying signal is experimentally de-aggregated onto two four-pulse amplitude modulation signals using nonlinear processes in optical elements. Quadrature-phase-shift-keying signals are similarly de-multiplexed into two binary phase shift keying signals by mapping the data points onto the constellation axes. De-multiplexing performance is evaluated as a function of the optical signal-to-noise ratio of the incoming signals. The effect of phase noise is also studied. © 2015 Optical Society of America

OCIS codes: (060.2360) Fiber optics links and subsystems; (190.4223) Nonlinear wave mixing.

<http://dx.doi.org/10.1364/OL.40.004899>

Reconfigurable and flexible optical networks have the potential to improve flexible spectral efficiency control and intelligent resource allocation. Aggregation of lower-capacity channels into a single higher-capacity channel and de-aggregation of a higher-capacity channel into many lower-capacity channels enable such flexibility in optical networks. These functions are critical because individual users rarely need the full bandwidth of a high-capacity network [1,2]. Aggregation and de-aggregation processes combined with the decision made by the control plane in the optical network could potentially be used to send bit streams with different bandwidths to different users. For a high-capacity optical network, aggregation and de-aggregation in the optical domain has important benefits: (i) avoiding inefficient optical-to-electrical conversions; (ii) supporting higher channel capacity; and (iii) achieving linear transformations over a wide dynamic range.

Phase-based data modulation formats, e.g., quadrature-phase-shift-keying (QPSK) or multi-level phase-shift-keying (M-PSK), are gaining importance in high-capacity optical

networks, which require their aggregation and de-aggregation. Optical aggregation has been demonstrated for higher-order phase-based modulation [3,4] as has optical de-aggregation of advanced modulation signals such as QPSK signals [5–11]. Optical QPSK de-aggregation has also been experimentally shown [5–10]. These approaches have typically required the use of a feedback loop to stabilize phase within the de-aggregator. Moreover, optical de-aggregation of higher-order modulation formats has been simulated [10,11] but there has been little published on experimental de-aggregation of higher-order phase-shift-keying (PSK signals). Further, optical de-aggregators were investigated to support other functions such as simplified receivers [12,13]. Thus it would be valuable to experimentally demonstrate optical de-aggregation of QPSK and higher-order PSK into multiple data channels of lower capacity without the need for feedback-based phase stabilization.

We experimentally demonstrate an optical channel de-aggregation for QPSK and 8-PSK data signals into lower-order signals by implementing the mapping process onto the constellation axes [14]. The process of mapping onto each of the axes uses a $\chi^{(3)}$ nonlinear element to generate a copy and a phase conjugate copy of the signal. In a subsequent $\chi^{(2)}$ nonlinear element, the phase conjugate copy of the signal is either added to or subtracted from the signal to achieve the mapping process onto each of the axes. A one-symbol time delay is introduced to maintain coherence and reduce phase noise without a feedback loop [15], which also transforms the input (and thus output) signal into a differential encoding. Optical signals with 8-PSK or QPSK formats are de-aggregated onto differential signals on lower capacity channels. A 20 Gbaud 8-PSK signal with an error vector magnitude (EVM) of 8.7% is mapped onto in-phase (I) and quadrature-phase (Q) components with 4-pulse amplitude modulation (PAM) formats and EVMs of 8.8%. To show bit-rate tunability, QPSK signals with EVMs of 9.5%

at baud rates of 30(20) Gbaud are experimentally de-aggregated onto I- and Q-parts as binary phase shift keying (BPSK) signals with EVMs of 11.4%. The system is also studied by changing the input optical signal-to-noise ratio (OSNR) and measuring the output EVM and OSNR. We also induce phase-noise on the input signal and at the output, to demonstrate that the phase-noise is also squeezed on the mapping axes.

Figure 1 shows the concept of the optical channel de-aggregator using mapping of the data information onto the constellation axes. The I-component of the result is generated by mapping the constellation points of the phase modulated signals, e.g., QPSK and 8-PSK, onto the I-axis by coherently adding the signal $s(t) = e^{j\phi_s(t)}$ with its conjugate, i.e., $I = s(t) + s^*(t) = e^{j\phi_s} + e^{-j\phi_s}$. The Q-component of the signal is generated by mapping the constellation onto Q-axis, i.e., $Q = s(t) - s^*(t) = e^{j\phi_s} - e^{-j\phi_s}$, [as shown in Figs. 1(a) and 1(b)]. To implement the mapping process optically, the block diagram shown in Fig. 2 is used. First, the input signal $s(t) = e^{j\phi_s(t)}$ (QPSK/8-PSK) at ω_s and two continuous-wave (CW) pumps with electrical fields of P_1 and P_2 at frequencies of ω_{p1} and ω_{p2} are sent through a $\chi^{(3)}$ nonlinear element [such as highly nonlinear fiber (HNLF)] to generate copies of the signal in a four-wave-mixing process. A copy with the field of $P_1 P_2^* s(t)$ at $\omega_{c1} = \omega_{p1} + \omega_s - \omega_{p2}$ and two conjugate copies of the signal with the fields of $P_1 P_2 s^*(t)$ and $P_2^* s^*(t)$ at $\omega_{c2} = \omega_{p1} + \omega_{p2} - \omega_s$ and $\omega_{c3} = 2\omega_{p2} - \omega_s$, respectively, are generated. Then, using a programmable delay and a phase and amplitude filter, the signals and copies are filtered and required delays and complex coefficients are induced. As shown in Fig. 2, one symbol-time (T) delay is introduced between the signal and

its conjugate. The delay is used to maintain coherence and remove noise in the signal and its conjugate, which enables de-aggregation without a feedback loop [15] at the cost of generating differentially-encoded outputs.

In the final stage, in a $\chi^{(2)}$ nonlinear element such as a periodically-poled-lithium-niobate (PPLN) waveguide, the differential of the input signal is coherently combined with its differential conjugate to implement the mapping process. Stated differently, using a PPLN waveguide with a quasi-phase matching (QPM) frequency of ω_{QPM} , which is tuned to be at the center of the signals and delayed signals, i.e., $\omega_s + \omega_{c2} = \omega_{c1} + \omega_{c3} = 2 \times \omega_{\text{QPM}}$, the conjugate copy of $P_1 P_2 s^*(t)$ at ω_{c2} mixes with the signal $s(t - T)$ at ω_s through a sum-frequency-generation process to create a signal at $2 \times \omega_{\text{QPM}}$ with a field proportional to $P_1 P_2 s^*(t) s(t - T)$. In the same process the copy of the signal $P_1 P_2^* s(t)$ at ω_{c1} mixes with the conjugate copy of the signal $P_2^* s^*(t - T)$ at ω_{c3} to create a signal at $2 \times \omega_{\text{QPM}}$ with a field proportional to $P_1 P_2^* s(t) P_2^* s^*(t - T) = P_1 P_2 s(t) s^*(t - T)$. The generated signal $A_{2\omega_{\text{QPM}}}$ at $2 \times \omega_{\text{QPM}}$ will be

$$\begin{aligned} A_{2\omega_{\text{QPM}}} &\propto P_1 P_2^* s(t) P_2^* s^*(t - T) + \alpha P_1 P_2 s^*(t) s(t - T) \\ &= P_1 P_2 s(t) s^*(t - T) + \alpha P_1 P_2 s^*(t) s(t - T) \\ &\propto s(t) s^*(t - T) + \alpha s^*(t) s(t - T) \\ &= e^{j\phi_s(t)} e^{-j\phi_s(t-T)} + \alpha e^{-j\phi_s(t)} e^{j\phi_s(t-T)} \\ &= e^{j[\phi_s(t) - \phi_s(t-T)]} + \alpha e^{-j[\phi_s(t) - \phi_s(t-T)]} \\ &= e^{j\Delta\phi_s(t)} + \alpha e^{-j\Delta\phi_s(t)}, \end{aligned} \quad (1)$$

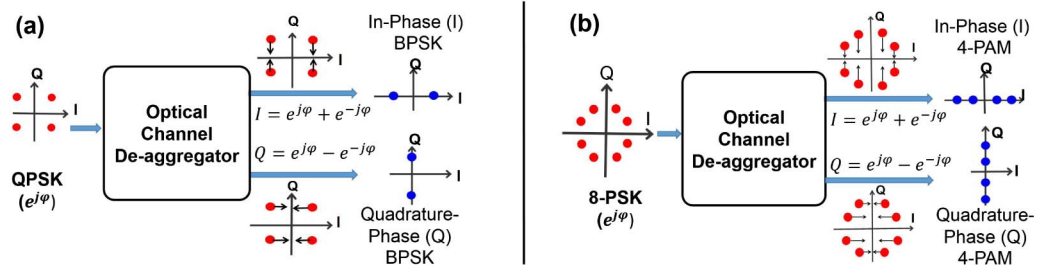


Fig. 1. Concept of the optical channel de-aggregator, (a) optical mapping of the QPSK signal onto I- and Q-axes to extract two BPSK signals and (b) optical de-multiplexing of an 8-PSK signal into two 4-PAM signals using mapping.

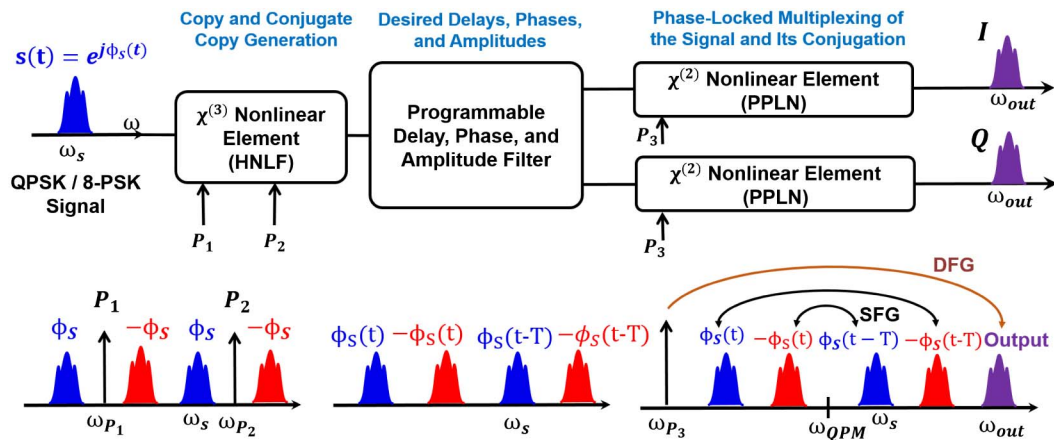


Fig. 2. Conceptual block diagram of the optical channel de-aggregator.

in which $\Delta\phi_s(t) = \phi_s(t) - \phi_s(t - T)$ is the differentiated version of the input QPSK/8-PSK signal. From Eq. (1), inside the programmable filter the coefficient α can be changed to map the signal onto different axes. To generate I/Q output for the I-component, we use $\alpha = 1 \angle 0$ and for the Q-part we use $\alpha = 1 \angle 180 = -1$ (shown in Fig. 2). Another pump laser at ω_{p3} is also injected into the PPLN waveguide to convert the generated signal at $2\omega_{QPM}$ back to the C-band frequency $\omega_{out} = 2\omega_{QPM} - \omega_{p3}$ through a difference-frequency-generation process. The output of the system is then sent to a coherent receiver to be analyzed. Using this method the differentiated version of the signal has thus been added to its conjugate, i.e., $e^{j[\phi(t) - \phi(t-T)]} + \alpha e^{-j[\phi(t) - \phi(t-T)]}$ to implement the optical de-aggregation of optical QPSK/8-PSK signals using mapping onto constellation axes. This approach is also tunable for different data baud rates because the induced one-symbol time delay can be adjusted as needed.

Figure 3(a) shows the experimental setup for the tunable optical-channel de-aggregator. At the transmitter a signal at $\lambda_s = 1548$ nm is modulated in a nested Mach-Zehnder modulator with 30 (20) Gbaud QPSK data (pseudo random bit sequence [PRBS] $2^{31} - 1$). A phase modulator driven in $V_\pi/8$ with a 10 Gb/s data (PRBS $2^{31} - 1$) is followed by the QPSK data transmitter to generate a 10 Gbaud 8-PSK signal. A variable optical attenuator followed by a preamplifier changes the OSNR of the input signal for different experimental configurations. Phase noise is injected using a phase modulator driven by random noise generated by a photodiode in order to study its impact on de-aggregator performance.

The generated QPSK/8-PSK signal is then sent to the optical channel de-aggregator. Two pumps at $\lambda_{p1} = 1547$ nm and $\lambda_{p2} = 1554$ nm, after being amplified are sent to the first nonlinear stage into a HNLf (450 m) to generate copies

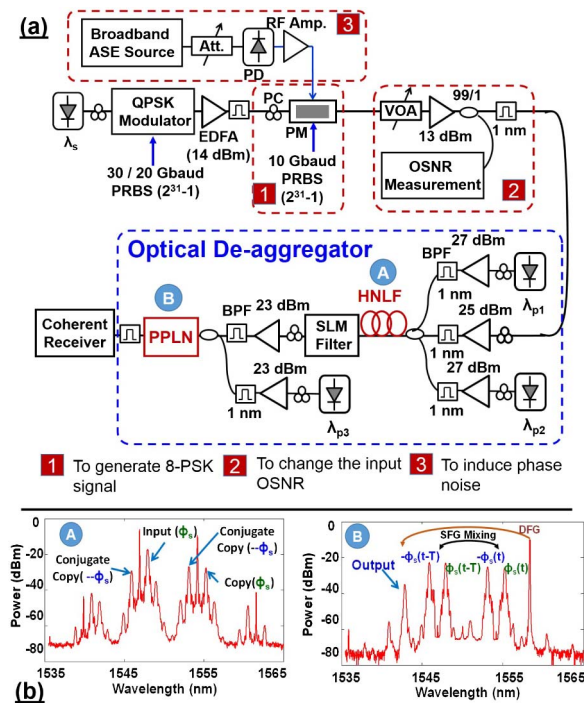


Fig. 3. (a) Experimental setup for optical channel de-aggregator PM, phase modulator; PC, polarization controller; EDFA, erbium doped fiber amplifier; VOA, variable optical attenuator and (b) optical spectra of the nonlinear stages.

[shown as (A) in Fig. 3(a)]. The optical spectrum of the output of HNLf is shown in Fig. 3(b). As measured from the spectrum, new generated signals have power levels around 13 dB less than the input signal, showing the conversion efficiency of the first stage. Using a spatial light-modulator filter as a programmable delay, phase, and amplitude filter, the signal and its copies are filtered and the desired delays are induced. The corresponding signals, together with another CW pump at $\lambda_{p3} = 1558$ nm, are sent through the second nonlinear stage in a ~ 4 -cm long PPLN waveguide to implement de-aggregation, whose spectrum is shown in Fig. 3(b) as (B). The conversion efficiency of $-14 \times$ dB is achieved for this stage. The QPM wavelength of the PPLN waveguide is temperature tuned to 1550.5 nm as the middle frequency between the signals and delayed ones. The output signal, shown in the figure, is then filtered and sent to the coherent receiver to be analyzed.

Figures 4(a)–4(c) show the constellations of the input QPSK and 8-PSK signals and the corresponding de-multiplexed (de-aggregated) signals. A 30 Gbaud QPSK signal with an EVM of 9.9% as an input to the system is de-aggregated into in-phase and quadrature-phase axes as BPSK signals with EVMs of $\sim 11.5\%$. Tunability over the baud rate is also shown by changing the baud rate of the QPSK signal to 20 Gb. The result is shown in Fig. 4(b). The setup is reconfigurable to the other phase modulated signals, as shown by de-aggregating a 20 Gbaud 8-PSK signal with an 8.7% signal into in-phase 4-PAM with an 8.9% EVM and quadrature-component 4-PAM signal with an 8.8% EVM. We study the de-aggregation setup by changing the OSNR of the incoming signal and measuring the de-aggregated signal quality. Figure 5 shows the quality of the de-multiplexed BPSK/4-PAM signals for the input QPSK/8-PSK signals at 30(20) Gbaud rates with different OSNR values. As shown in Fig. 5(a), input and output OSNR relate linearly in the dB scale in the lower OSNR region. By increasing the input OSNR, the output OSNR increases, and at high-input OSNR, saturation in the OSNR of de-aggregated signal is observed. We believe this behavior is due to the limited input power that can be inserted into the PPLN waveguide, which is 100 mW. This limitation, along with the PPLN conversion efficiency, constrains the signal-power level at the output and its OSNR. Additionally, the noise of high-power EDFAs has a potential impact on system performance by limiting the maximum possible OSNR at the output. Figure 5(b) shows the EVM of the output differential BPSK signals versus the input QPSK signal OSNR.

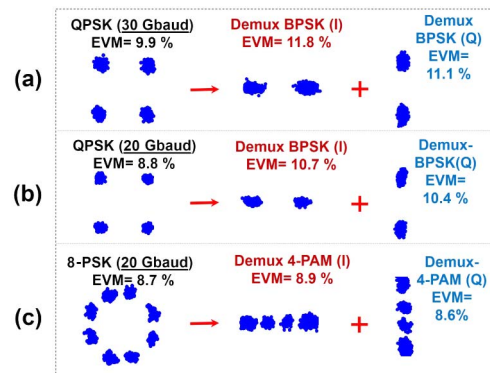


Fig. 4. Experimental results of 20 Gbaud 8-PSK and 30(20) Gbaud QPSK signal de-aggregation.

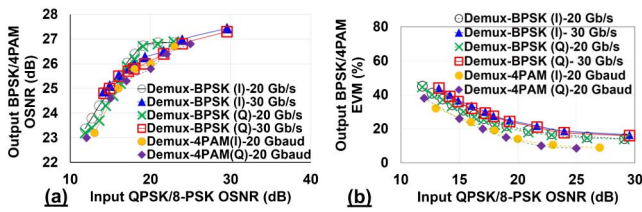


Fig. 5. (a) OSNR and (b) EVM of the de-multiplexed BPSK signals versus input QPSK signal OSNR at 30(20) Gbaud.

values. For the input signal with lower OSNR, the EVM of the output BPSK signal is increased.

We also investigate the system performance by varying the phase noise values of the input signal. Figure 6(a) shows the constellation of the incoming QPSK signals with different values of phase noise and corresponding de-multiplexed I- and Q-BPSK signals. As shown, the phase noise of the signal is mapped and squeezed on the constellation axes. For different values of phase noise, the output BPSK total phase values are measured and shown in Fig. 6(b). Thus, the de-aggregation setup based on the mapping onto constellation axes converts the optical input phase noise to the amplitude noise. It should be noted that the mapping process converts the phase noise with amplitudes up to 70 deg to the 20 deg phase noise on the axes. Furthermore, in order to reduce the amplitude noise, an amplitude saturation stage could potentially be used at the output [15]. Moreover, we used narrow linewidth (10 kHz) lasers for the pumps in the setup because the phase noise due to the linewidth of the lasers would be added to the output and could set a limitation on the system performance [15,16]. Finally, we measure the bit error rate (BER) for the input and de-aggregated differential output signals using the EVM measurements as shown in Fig. 7. At BER of 1e-3, ~3 dB OSNR difference between OSNR of the input QPSK signals and output BPSK signals is measured.

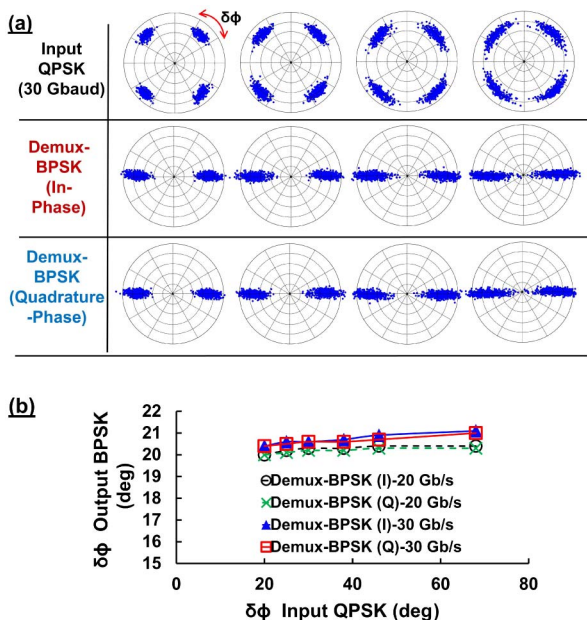


Fig. 6. (a) Constellations for the input QPSK with phase noise and de-multiplexed BPSK signals. (b) Measured total phase of the output BPSK signals versus total phase of the QPSK signal.

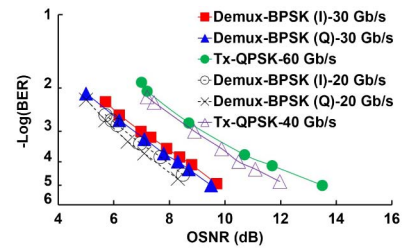


Fig. 7. BER measurements of the input and output.

In conclusion, optical channel de-aggregation of M -array PSK signals for $M = 4, 8$ is implemented by mapping onto the constellation axes. Inducing a one symbol time delay achieves the required coherence of the mapping function and reduces output phase noise without feedback-based phase stabilization at the expense of converting the output into a differential encoding. System performance is investigated by studying the output signal quality for different input OSNR values and BER measurements. The squeezing of the mapping process onto the constellation is shown by varying the phase noise of the incoming signal and measuring the output phase noise.

Funding. Center for Integrated Access Network (CIAN); National Science Foundation (NSF).

REFERENCES

- S. Sygletos, I. Tomkos, and J. Leuthold, *J. Opt. Commun. Netw.* **7**, 321 (2008).
- O. Gerstel, M. Jinno, A. Lord, and S. Yoo, *IEEE Commun. Mag.* **50**(2), s12 (2012).
- M. R. Chitgarha, S. Khaleghi, Z. Bakhtiari, M. Ziyadi, O. Gerstel, L. Paraschis, C. Langrock, M. M. Fejer, and A. E. Willner, *Opt. Lett.* **38**, 3350 (2013).
- G.-W. Lu, T. Sakamoto, and T. Kawanishi, *Opt. Express* **21**, 6213 (2013).
- F. Da Ros, K. Dalgaard, Y. Fukuchi, J. Xu, M. Gallii, and C. Peucheret, *IEEE Photon. Technol. Lett.* **26**, 1207 (2014).
- A. Lorences-Riesgo, F. Chiarello, C. Lundström, M. Karlsson, and P. A. Andrekson, *Opt. Express* **22**, 21889 (2014).
- R. P. Webb, M. Power, and R. J. Manning, *Opt. Express* **21**, 12713 (2013).
- M. Gao, T. Kurosu, T. Inoue, and S. Namiki, *European Conference on Optical Communication (ECOC)* (2013), paper We.3.A.5.
- N.-K. Kjoller, M. Gallii, K. Dalgaard, H. Mulvad, K. Roge, and L. Oxen-Howe, *European Conference on Optical Communication (ECOC)* (2014), paper P.3.8.
- F. Parmigiani, G. Hesketh, R. Slavík, P. Horak, P. Petropoulos, and D. J. Richardson, *J. Lightwave Technol.* **33**, 1166 (2015).
- A. Bogris, *Opt. Lett.* **39**, 1775 (2014).
- M. Gao, T. Kurosu, T. Inoue, and S. Namiki, *OptoElectronics and Communications Conference and Photonics in Switching (OECC/PS)* (2013), paper TuS2-4.
- F. Da Ros, J. Xu, L. Lei, and C. Peucheret, *OptoElectronics and Communications Conference and Photonics in Switching (OECC/PS)* (2013), paper TuS2-5.
- M. Ziyadi, A. Mohajerin-Ariaei, M. Chitgarha, Y. Cao, S. Khaleghi, A. Almairan, J. Touch, L. Paraschis, M. Tur, C. Langrock, M. M. Fejer, and A. Willner, *European Conference on Optical Communication (ECOC)* (2014), paper P.3.18.
- A. Mohajerin-Ariaei, M. Ziyadi, M. R. Chitgarha, A. Almairan, Y. Cao, B. Shamee, J.-Y. Yang, Y. Akasaka, M. Sekiya, S. Takasaka, R. Sugizaki, J. D. Touch, M. Tur, C. Langrock, M. M. Fejer, and A. E. Willner, *Opt. Lett.* **40**, 3328 (2015).
- R. Hui and A. Mecozzi, *Appl. Phys. Lett.* **60**, 2454 (1992).